

# Energy focusing inside a dynamical cavity

K. Colanero and M. -C. Chu

*Department of Physics, The Chinese University of Hong Kong, Shatin, N.T., Hong Kong.*

We study the exact classical solutions for a real scalar field inside a cavity with a wall whose motion is self-consistently determined by the pressure of the field itself. We find that, regardless of the system parameters, the long-time solution *always* becomes nonadiabatic and the field's energy concentrates into narrow peaks, which we explain by means of a simple mechanical system. We point out implications for the quantized theory.

The dynamics of confined cavity fields interacting with the cavity wall is of great interest for the understanding of a variety of problems such as hadron bag models [1], sonoluminescence [2], cavity QED [3] and black hole radiations [4]. Previous works have mostly approached the problem assuming an externally imposed wall motion, neglecting the effects of the radiation pressure, or used the adiabatic approximation [5,6]. In this paper we study, without any approximation, the dynamics of a real scalar field inside a cavity, the wall of which moves according to the combined force of a static potential  $V(R)$  and the field pressure. This system bears important resemblances to more complicated ones, such as the Dirac and electromagnetic fields, since they can be partially or completely cast in the form of a wave equation. Moreover the classical solutions should be a good approximation to the quantized fields at least in the case of a large number of field quanta. As initial condition for the field we always consider a normal mode of the static cavity. This is in fact a common situation in the study of many physical systems.

We find that in general the system evolves nonadiabatically, and the field energy concentrates into narrow peaks. This phenomenon can be understood with the help of a simple classical mechanical system.

In the present work we use natural units and hence the action  $\mathcal{S}$  is dimensionless as are the velocities. This simply means that, although we are dealing with a classical system, for convenience the action is taken in units of  $\hbar$ . In one space dimension and with the field only inside the cavity, the system is defined by the action

$$\mathcal{S} = \int_0^t dt' \left\{ \frac{1}{2} M \dot{R}^2 - V(R) + \int_0^R dx \frac{1}{2} [\phi_{t'}^2 - \phi_x^2] \right\}. \quad (1)$$

Imposing  $\delta\mathcal{S} = 0$  under any variation of the dynamical variables that vanishes at  $t' = 0$  and  $t' = t$  we obtain:

$$M\ddot{R} + \frac{\partial V(R)}{\partial R} - \frac{1}{2} [\phi_t^2 - \phi_x^2]_{x=R} = 0, \quad (2)$$

$$\phi_{tt} - \phi_{xx} = 0 \quad 0 \leq x < R, \quad (3)$$

$$\begin{aligned} \phi_x &= 0 & \text{at } x = 0, \\ \phi_x &= -\dot{R}\phi_t & \text{at } x = R. \end{aligned} \quad (4)$$

Notice the dependence on  $\dot{R}$  of the boundary conditions. If  $\phi(R) = 0$  is imposed, the total energy, which is conserved for a static cavity, is no longer constant for  $\dot{R} \neq 0$ . Eq. 3 is satisfied by  $\phi(x, t)$  with

$$\phi(x, t) = G(t - x) + G(t + x) \quad (5)$$

and the positive sign between the two  $G$ 's ensures that the first boundary condition of Eqs. 4 is met. Substituting Eq. 5 in the second of Eqs. 4 we obtain:

$$G'(t + R(t)) = \frac{1 - \dot{R}(t)}{1 + \dot{R}(t)} G'(t - R(t)). \quad (6)$$

For prescribed wall motion,  $G(z)$  for any  $z$  can be found by using Eq. 6 and the null line method [5]. It is assumed that the cavity is static for  $t \leq t_0$  with a length  $R(t_0)$ . This is equivalent to saying that there is a static zone  $z \leq z_0 = t_0 + R(t_0)$ , in which  $G(z)$  is analytically known. One can find the values of  $G(z > z_0)$  outside the static zone by first solving the algebraic equation  $z = t_{\text{eqv}} + R(t_{\text{eqv}})$  for  $t_{\text{eqv}}$  and then finding  $z_- \equiv t_{\text{eqv}} - R(t_{\text{eqv}})$ . This process, which is equivalent to constructing a null line connecting the points  $z$  and  $z_-$ , can be repeated many times until a point  $z_s$  in the static zone is reached. The values of  $G(z)$  and  $G(z_s)$  are related through Eq. 6. However in the case under study, we do not have, in general, a static zone, and we need to verify that knowing the initial conditions of the system is enough to implement the above method.

We will show that in order to find  $\phi(x, t + dt)$  with  $0 \leq x \leq R(t + dt)$ , it is necessary and sufficient to know  $G(z)$  and  $G'(z)$  for  $t - R(t) \leq z \leq t + R(t)$  and  $R(t')$  for  $t \leq t' \leq t + dt$ . That is just what is required in order to have a unique solution of the system of two second order equations (2) and (3).

Since  $\phi(x, t + dt) = G(t + dt - x) + G(t + dt + x)$ , we need to find  $G(z)$  and  $G'(z)$  for  $t + dt - R(t + dt) \leq z \leq t + dt + R(t + dt)$ . Now we have two cases: either  $z \leq t + R(t)$  or  $z > t + R(t)$ .

In the first case it is also true that

$$z \geq t + dt - R(t + dt) \geq t - R(t)$$

as long as  $\dot{R} \leq 1$ , *i.e.* in all physical situations, so that we already have the solution.

In the second case we have to solve the equation  $z = t_{\text{eqv}} + R(t_{\text{eqv}})$ , as explained previously. We have

$$t + R(t) \leq t_{\text{eqv}} + R(t_{\text{eqv}}) \leq t + dt + R(t + dt),$$

which, with  $\dot{R} \geq -1$ , implies

$$t \leq t_{\text{eqv}} \leq t + dt.$$

Having found  $t_{\text{eqv}}$  we can derive  $G'(z)$  from Eq. 6 because, with  $z_{\text{eqv}} \equiv t_{\text{eqv}} - R(t_{\text{eqv}})$ ,

$$t - R(t) \leq z_{\text{eqv}} \leq t + R(t) \quad |\dot{R}| \leq 1 ,$$

so that again we have the necessary information to determine the evolution of the field.  $G(z)$  can then be obtained by the numerical integration of  $G'(z)$ . Note however that while  $\dot{R} = 1$  still admits a solution for the field,  $\dot{R} = -1$  doesn't, because the boundary condition requires  $G'(t + dt - R(t + dt)) = G'(t + 2dt - R(t)) = 0$ , which in general is inconsistent. Evolving backward in time, *i.e.* with  $dt < 0$ , the opposite would be true.

Using the procedure above we have studied the case with  $V(R) = \frac{1}{2}K(R - R_0)^2$ , solving, step by step, Eq. 2 numerically by a standard finite difference method.

As initial condition for the field we choose the fundamental mode of the static cavity with Eqs. 4 as the b.c.,  $R(t_0) = R_0$ , and  $\dot{R}(t_0) = 0$ :

$$\begin{cases} \phi = \sin \omega t_0 \cos \omega x , \\ \phi_t = \omega \cos \omega t_0 \cos \omega x , \end{cases} \quad w \equiv \frac{\pi}{R_0} . \quad (7)$$

For convenience we define the dimensionless parameters  $\alpha$  and  $\beta$ :  $\alpha \equiv M/\omega$ ,  $\beta \equiv \Omega/\omega = \sqrt{K/M}/\omega$ , and we set the amplitude of the initial field to be 1. In the case of a wall initially at rest and with a large mass compared to the initial energy of the field, we expect the dynamics not to depart considerably from the adiabatic one, that is, the wall's motion should be well approximated by the solution of Eq. 2, with the field's pressure term replaced by its static wall counterpart and the solution of Eq. 3 by

$$\phi(x, t) = \sin \omega(t)t \cos \omega(t)x \quad w(t) \equiv \frac{\pi}{R(t)} . \quad (8)$$

In order to check the reliability of our numerical implementation of the algorithm, we first considered a large mass of the wall ( $\alpha = 1000/\pi$ ,  $\beta = 1/(10\pi\sqrt{2})$ ). We verified that the total energy is very well conserved and the motion of the wall is well reproduced by the solution of Eq. 2 with the static wall solution for the field pressure.

We then used a smaller mass keeping  $K$  constant, *i.e.*  $\alpha = 100/\pi$  and  $\beta = 1/(\pi\sqrt{20})$ . As shown in Fig. 1, both the wall motion and the field energy density become nontrivial. An interesting feature is the concentration of the energy density, shown in Fig. 1c. This is confirmed by the plot of the energy density at two instances  $t = 349R(t_0)$  and  $t = 697R(t_0)$  in Fig. 2 compared with the static cavity solution. The two peaks at  $t = 697R(t_0)$  move in opposite directions, and their widths decrease in time. This phenomenon is even more evident with  $\alpha = 10/\pi$  and  $\beta = 1/(\pi\sqrt{2})$  (Fig. 3a), showing a complex distribution of the peak locations and heights. The total energy of the system is the same in all cases.

Even for the case in Fig. 3b ( $\alpha = 1000/\pi$ ,  $\beta = 1/(10\pi\sqrt{2})$ ), for which we observed the adiabatic evolution lasting for a long time after  $t_0$ , we can still, letting the system evolve long enough, observe the squeezing of the field energy density in spite of the slow motion of the wall. Keeping  $K$  constant we found that the time at which the focusing of the energy starts increases roughly linearly with  $M$ . This suggests that, as one takes into account the backreaction of the field on the wall motion, the long-time dynamics always becomes nonadiabatic. We have verified that this remains true also changing the boundary conditions so that the field equals zero at the boundaries.

We believe that the origin of this phenomenon lies in the mechanism of energy exchange between the wall and the field. To explain it we give the following qualitative argument. Let's consider the interaction between the wave inside the cavity and the wall. At some instance, the peak of the wave will hit the wall, which can be moving either outward or inward. In the former case, there will be a transfer of energy from the field to the wall, and the speed of the wall will increase slightly. The wavefronts following the peak will lose more and more energy to the wall, since the wall moves faster with each successive collision. As a result the spatial width of the energy distribution decreases. When the wall moves inward, the wave gains energy from the wall, and the wavefronts following the peak gain less because the wall moves slower with each successive collision. Again the width of the waveform decreases. After some time, this effect leads to a drastic concentration of energy into narrow peaks.

Our argument depends only on kinematics and should therefore be applicable not only to waves but many other systems, such as a set of particles bouncing back and forth in a dynamical cavity. For simplicity we consider the dynamics of a set of massless non-interacting particles, each having momentum and energy  $p_i$ ,  $|p_i|$  ( $c = 1$ ). Inside the cavity they move unperturbed at the speed of light. If a particle bounces on the static wall, its momentum changes sign. The movable wall is subjected to a harmonic potential  $V(R) = \frac{1}{2}K(R - R_0)^2$ . The particle momentum  $p_i''$  and the wall velocity  $v''$  after an interaction, which is assumed to be instantaneous, are easily

derived from energy and momentum conservation:

$$\begin{aligned} v'' &= \sqrt{(1+v')^2 + 4p'/M} - 1 \quad , \\ p'' &= p' + M(v' - v'') \quad , \end{aligned} \quad (9)$$

where  $v'$  and  $p'$  are the wall velocity and particle momentum before the collision. The above equations are derived assuming that the sign of  $p''$  is always opposite to the sign of  $p'$ , which is true as long as the speed of the wall is less than 1 and  $2M(1-v') > p'$  ( $p' > 0$ ).

We consider first a set of 1000 particles all with the same initial momentum  $p_i = 0.01/R(t_0)$  and a wall initially at rest with  $M = 1000/R(t_0)$  and  $\Omega = 1/R(t_0)$ . Already after a few interactions with the wall we could observe a regular transfer of energy from the last to the first particles to hit the wall. In Fig. 4a we show the momenta of the particles after a time  $t = 3221R(t_0)$  as a function of their position. For clarity only positive momenta are plotted. It is remarkable that the first particle to hit the wall has gained more than one tenth of the total energy of the system. The above is a very special situation which however demonstrates the process of energy transfer among particles.

We then extend this simple mechanical model to the case of an infinite number of particles labeled with a continuous index  $k$ , each having position  $q(k)$  and momentum  $p(k)dk$ . In this way we can define an energy density:

$$\mathcal{E}(x, t) \equiv \int dk |p(k, t)| \delta(q(k, t) - x) \quad . \quad (10)$$

Not surprisingly  $\mathcal{E}(x, t)$  satisfies the wave equation inside the cavity. We numerically simulate such a system choosing 2000 particles. Initially, we put two particles at each of the 1000 uniformly separated sites, and the pairs have opposite momenta  $p(k) = \pm 10(\pi^2 \cos^2 \pi q(k) + 1)$ . In Fig. 4b we plot  $\mathcal{E}(0, t)R^2(t)$ , which is evidently similar to Fig. 1, although the details of the evolution depend on how the particles or the field interact with the wall.

After a long time we observe the formation of many smaller peaks in the energy density. Further work is needed to understand the problem of the  $t \rightarrow \infty$  evolution of the system.

For the scalar field an important situation to study is when  $\Omega = \pi/R_0$ , *i.e.*, when the wall motion is in resonance with the field inside the cavity. We have computed the solutions of Eqs. 2 and 3 for various masses of the wall. In Fig. 5 we plot the wall's position and the field energy density at  $x = 0$  vs. time in the case of  $\alpha = 1000/\pi$ ,  $R(t_0) = R_0$  and  $\dot{R}(t_0) = 0.1$ . In this case we choose  $t_0 = R_0/2$  so that  $\dot{\phi} = 0$  and the initial functions Eq. 7 satisfy the boundary condition Eqs. 4 with  $\dot{R}(t_0) \neq 0$ . Besides the beats in the wall motion, two features are important. One is the fact that the wall continues to return to its initial position after a time  $T = R_0$ . This is different from the case of non-resonant wall parameters where the back reaction of the field changes the frequency

of the wall motion. Another remarkable effect, as a consequence, is the appearance of narrow peaks typical of a resonantly driven wall motion [5,7,9]. This indicates the possibility of transferring a large amount of energy to the field even with an *external, non-resonant, driving force* [8,10]. As long as the frequency of the cavity wall is  $\Omega = \pi/R_0$ , it is enough to push the wall at the instances marked by the arrows in Fig. 5, and this frequency depends on the mass of the wall and can be much smaller than  $\Omega$ ; increasing the mass decreases the frequency of energy exchange between wall and field. This fact might help to by-pass the experimental difficulty of achieving a resonant driving force, *i.e.* at frequency  $\Omega$ , on a mirror in order to produce high frequency photons [8].

We have verified that for a small mass,  $\alpha = 10/\pi$ , the wall period remains close to  $T = 2R_0$  so that the motion is still resonant [7].

In Ref. [7] it has been shown that the method of null lines can also be applied to waves inside an oscillating *spherical* cavity for any value of the angular momentum. However, when considering a self-consistent wall motion, the spherical symmetry is achieved only in the case of s-waves, for which the radial ( $\phi$ ) and angular parts can be separated. Defining  $\psi \equiv r\phi$ , so that  $\psi$  satisfies the one-dimensional wave equation, we can apply the null lines method. The boundary condition for  $\phi$ , derived from the action similarly to Eqs. 4, is:

$$\dot{R}\phi_t(R(t), t) = -\phi_r(R(t), t) \quad , \quad (11)$$

which however for  $\psi$  translates to:

$$\dot{R}\psi_t(R(t), t) = \frac{\psi(R(t), t)}{R(t)} - \psi_r(R(t), t) \quad . \quad (12)$$

If we want  $\phi$  to be finite at  $r = 0$  then we must require  $\psi = 0$  at  $r = 0$ , which is satisfied by writing  $\psi = G(t-r) - G(t+r)$ . Eq. 12 becomes:

$$\begin{aligned} G'(t+R(t)) - \eta G(t+R(t)) \\ = \gamma = -\frac{1-\dot{R}}{1+R} G'(t-R(t)) - \eta G(t-R(t)) \quad , \end{aligned} \quad (13)$$

with  $\eta \equiv 1/R(1+\dot{R})$ . An effective way to solve Eq. 13 *numerically* for  $G(t+R(t))$  is to define  $z = t+R(t)$  and to approximate  $\eta$  and  $\gamma$  with a constant value between  $z$  and  $z-dz$  for a small enough  $dz$ . Integrating Eq. 13 between  $z$  and  $z-dz$  we obtain:

$$G(z) = \left[ G(z-dz) + \frac{\gamma}{\eta} \right] e^{\eta dz} - \frac{\gamma}{\eta} \quad , \quad (14)$$

which turns out to be more accurate than standard numerical integration.

The force of the s-wave field on the wall is  $F_\phi = 2\pi R^2(t) [\phi_t^2 - \phi_r^2]$ . For  $\dot{R}(t_0) = 0$  we set as initial conditions for the fields:

$$\begin{cases} \phi(r, t_0) = \frac{\cos \omega t_0 \sin \omega r}{R_0^2 \omega r}, \\ \phi_t(r, t_0) = -\frac{\omega \sin \omega t_0 \sin \omega r}{R_0^2 \omega r}, \end{cases} \quad (15)$$

where  $\omega \simeq 4.4934/R(t_0)$  is chosen such that  $\phi(r, t_0)$  satisfies Eq. 11 with  $\dot{R}(t) = 0$ . As in the 1D case, we observe the formation of high energy density regions, although in 3D, this process is much slower. In Fig. 6 we plot the energy density at  $r = R(t)$  vs. time for  $\alpha = 5/4.4934$  and  $\beta = \sqrt{8}/4.4934$ . These values of the parameters produce a completely non-adiabatic evolution. For larger  $M$  or smaller  $K$  we have to evolve the system for a much longer time in order to observe the formation of high energy peaks. However we have verified that imposing  $\phi = 0$  at  $r = R(t)$  the peaks appear much earlier and the dynamics is very similar to the one-dimensional situation. With resonant wall parameters,  $\Omega = \pi/R(t_0)$ , the features observed in 1D remain in 3D. With the b.c. Eq. 11 it is also possible to have resonances with  $\Omega$  equal to the difference between the frequencies of the  $n^{\text{th}}$  mode and the fundamental mode of the cavity. However such an  $\Omega$  is close to  $n\pi/R(t_0)$  if  $n$  is large, and such resonances are not easily distinguishable from the geometric ones [7].

In summary we have applied the null lines method to study the dynamics of a scalar field inside a cavity whose wall is subjected to a harmonic force and the pressure due to the scalar field. We have found that the long time evolution of the system is always non-adiabatic, regardless of the parameters of the system. In particular there is an interval of time when the field develops narrow packets in energy density that bounce back and forth inside the cavity, which can be understood by means of a simple mechanical analog consisting of a set of massless particles bouncing inside a one-dimensional box with a movable wall. Such a system confirms our hypothesis that the wall motion provides a mechanism of energy transfer from low to high energy regions. We have verified that the focusing of energy is a robust phenomenon, being insensitive to the type of potential for the wall and the presence of an external driving force.

For a quantized field previous works [8] have shown that in the case of a prescribed slow wall motion no photon production is achieved. Our results strongly suggest that the back-reaction of the field may change significantly the evolution of the system. In particular the second derivative of the wall position, which is one of the quantities that determine the number of quanta [8], can be much larger than in the adiabatic case, as it can be seen from the slope of  $\dot{R}$  in Fig.1. If the initial number of fundamental mode quanta is large, the peaks in energy density in the classical solution can imply the production of several high energy quanta.

We have also studied the special situation in which the wall frequency is equal to the fundamental frequency of the static cavity field. Remarkably the frequency of the wall motion does not change due to the field pressure, and thus narrow peaks typical of a resonantly driven wall

motion are produced. A large amount of energy may be transferred to the field by providing mechanical energy to the wall when the amplitude of the oscillation reaches its minimum. This fact might help to by-pass the experimental difficulty of achieving a resonant driving force on a mirror in order to produce high frequency photons [8].

In a further work we would like to address the problem of whether periodical solutions are admitted for this kind of system and for which values of parameters.

We would like to thank Dr. C. K. Law for his interest in the paper and valuable discussions. This work is partially supported by a Hong Kong Research Grants Council grant CUHK 312/96P and a Chinese University Direct Grant (Project ID: 2060093).

- 
- [1] P. Hasenfratz and J. Kuti, Phys. Rep. **40**, 75 (1978).
  - [2] B. P. Barber *et al.*, Phys. Rep. **281**, 65 (1997), and references therein.
  - [3] G. T. Moore, J. Math. Phys. **11**, 2679 (1970); P. W. Milonni, *The Quantum Vacuum* (Academic Press, New York, 1993); N. D. Birrell and P. C. W. Davies, *Quantum Fields in Curved Space* (Cambridge University Press, Cambridge, 1982).
  - [4] S. W. Hawking, Nature **248**, 30 (1974); Commun. Math. Phys. **43**, 199 (1975).
  - [5] C. K. Cole and W. C. Schieve, Phys. Rev. A **52**, 4405 (1995), and references therein.
  - [6] P. Meystre *et al.*, J. Opt. Soc. Am. B **2**, 1830 (1985)
  - [7] K. W. Chan, U. M. Ho, P. T. Leung, and M.-C. Chu, The Chinese University of Hong Kong Preprint, 2000 (unpublished); K. W. Chan, Master Thesis, The Chinese University of Hong Kong (unpublished), 1999.
  - [8] V. V. Dodonov and A. B. Klimov, Phys. Rev. A **53**, 2664 (1996), and references therein.
  - [9] C. K. Law, Phys. Rev. Lett. **73**, 1931 (1994).
  - [10] A. Lambrecht, M. T. Jaekel and S. Reynaud, Phys. Rev. Lett. **77**, 615 (1996).

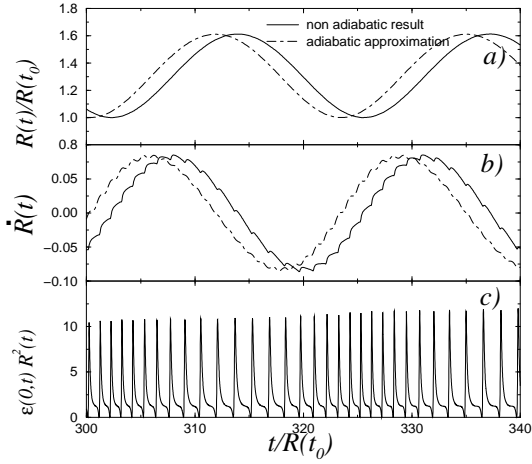


FIG. 1. a) Wall position, b) wall velocity, c) energy density of the field at  $x = 0$  for  $\alpha = 100/\pi$ ,  $\beta = 1/(\pi\sqrt{20})$ .

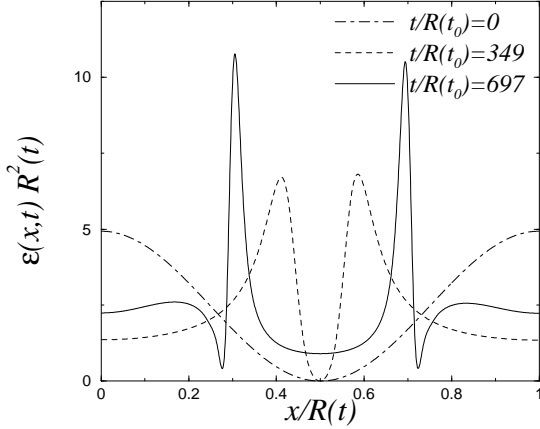


FIG. 2. Spatial distribution of energy density at  $t/R(t_0) = 0$  (dot-dashed), 349 (dashed line), and 697 (solid line) for  $\alpha = 100/\pi$ ,  $\beta = 1/(\pi\sqrt{20})$ .

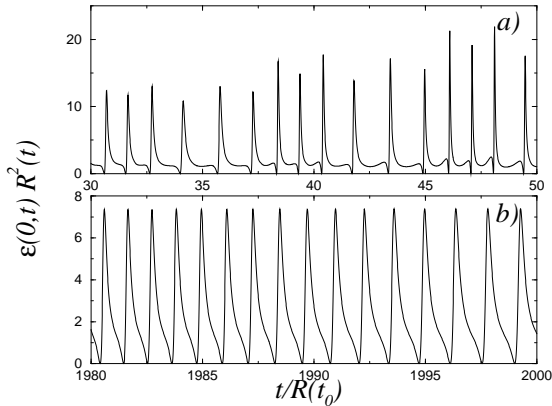


FIG. 3. Energy density of the field at  $x = 0$  for: a)  $\alpha = 10/\pi$ ,  $\beta = 1/(\pi\sqrt{2})$ , b)  $\alpha = 1000/\pi$ ,  $\beta = 1/(10\pi\sqrt{2})$ . Notice the time intervals.

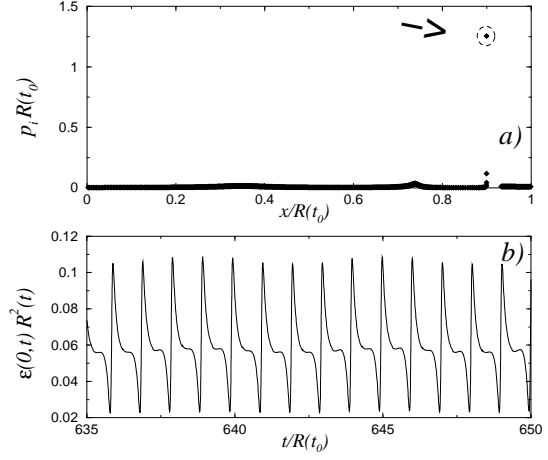


FIG. 4. Classical particles in a dynamical cavity, with  $M = 1000/R(t_0)$ ,  $\Omega = 1/R(t_0)$ , and initial momenta  $0.01/R(t_0)$ . a) Particle momenta at  $t = 3221R(t_0)$ . b) Generalized energy density at  $x = 0$ .

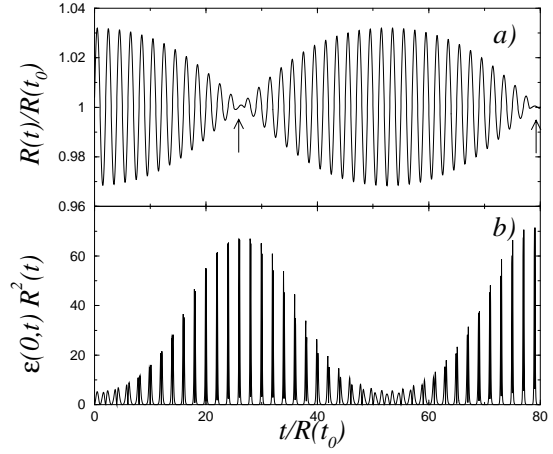


FIG. 5. a) Wall position and b) energy density in a resonant cavity with  $\alpha = 1000/\pi$  and  $\beta = 1$ .

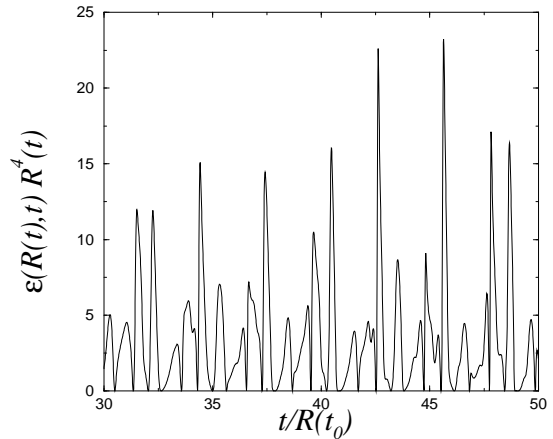


FIG. 6. Energy density in a spherical cavity at  $r = R(t)$  vs. time for  $\alpha = 5/4.4934$  and  $\beta = \sqrt{8}/4.4934$ .